

OPEN ACCESS

Occurrence of the vortex state for magnetic phase plates

To cite this article: M K Hari *et al* 2010 *J. Phys.: Conf. Ser.* **241** 012069

View the [article online](#) for updates and enhancements.

You may also like

- [Characteristics and controllability of vortices in ferromagnetics, ferroelectrics, and multiferroics](#)
Yue Zheng and W J Chen
- [On the optimal conditions for the formation and observation of long icosahedral nanowires of aluminium, nickel and copper](#)
P García-Mochales, S Peláez, P A Serena et al.
- [Fast switching of magnetic vortex state under an alternating magnetic field](#)
Min Xu, Guiqian Jiang, Zhiyu Zhang et al.



243rd Meeting with SOFC-XVIII

Boston, MA • May 28 – June 2, 2023

Accelerate scientific discovery!

[Learn More & Register](#)



Occurrence of the vortex state for magnetic phase plates

M K Hari, M Beleggia^{1,2}, R M D Brydson

Institute for Materials Research, University of Leeds, Leeds LS2 9JT, UK

E-mail: mb@cen.dtu.dk

Abstract. Tunable magnetic phase plates may be realized as nanorings magnetized in the vortex state, where tunability would be granted by the temperature dependence of the saturation magnetization. Here, we study the statistical occurrence of the magnetic vortex state in circular and pentagonal rings within their magnetic phase diagram. We outline the useful operational range of parameters that may be utilized in practice.

1. Introduction

In addition to a large number of promising applications in the field of magnetic memories [1] and spintronics [2], nanorings may be utilized as magnetic phase plates in electron microscopy to achieve Zernike-type phase contrast [3,4]. In fact, thanks to the Aharonov-Bohm effect experienced by the electrons traveling through a nanoring in the vortex state, a phase shift is induced between the transmitted and scattered beams. The main benefit is visible in-focus contrast associated with weak (or strong) phase objects such as biological samples [5]. Furthermore, it was hinted in [6] that employing Zernike mode may also result in a substantial decrease of the electron dose necessary to image single atoms or molecules, so that imaging radiation sensitive materials becomes more practical.

Aiming at the development of magnetic phase plates we focus here on the stability region of the vortex state in rings within a suitable parameter space. This is a necessary preliminary step to ascertain the range of dimensions and shapes that are compatible with an operational phase plate. Furthermore, we analyze with micromagnetic simulations the statistics of obtaining a vortex from a random initial configuration, and how the statistics varies with shape and size. This is useful to select the appropriate parameters that results in more frequent vortex states and, hence, reliable operability.

2. The phase shift of a magnetic phase plate

The vortex state is the sought magnetization state in the ring as it can induce the correct phase shift between the transmitted and scattered beam. The phase shift associated with a ring in the vortex state can be calculated from the standard expression [7] linking it to the magnetic vector potential

$$\varphi(r) = -\frac{\pi}{\phi_0} \int_{-\infty}^{+\infty} A_z(r, z) dz = N\pi \begin{cases} 1 & r < \bar{R} \\ 0 & r > \bar{R} \end{cases} \quad (1)$$

where $\phi_0 = 2.07 \times 10^{-15}$ T m² is the flux quantum, and we adopted a simplified description of a ring of thickness t and radii R_2 (outer) and R_1 (inner) as a circular flux line of radius \bar{R} carrying N flux quanta

¹ To whom any correspondence should be addressed.

² Now at: Center for Electron Nanoscopy, Technical University of Denmark, DK-2800 Kgs. Lyngby, Denmark.

(see Fig. 1). The phase shift described by equation (1) is what is required to achieve Zernike-type phase contrast: a constant phase equal to zero outside the ring (leaving the scattered electrons unperturbed), and another constant phase equal to $\phi_Z = N\pi$ (N times the phase shift of a flux quantum) inside the ring (inducing a shift to the transmitted electrons). If the vorticity of the ring changes, the phase shift within the inner radius of the ring changes sign, producing “negative” phase contrast.

3. Tunability with temperature and geometrical constraints

As discussed in [8], in electron microscopy the quarter-wavelength phase shift typical of light optics may not always be the optimal choice, as it is only appropriate for weak phase objects. Furthermore, even under controlled growth, we can never be sure *a priori* that the thickness of magnetic material is exactly what is needed to realize the Zernike shift we seek. Hence, tunability of the phase plate is a necessity. While electrostatic phase plates [9] are tunable by controlling some applied voltage, in magnetic phase plates one possibility is to operate the device at different temperatures. In fact, as illustrated above, the Zernike phase shift induced on the electrons is proportional to N , the number of flux quanta enclosed in the ring. Since N is the ratio between the magnetic flux and the flux quantum, and the magnetic flux is the product of magnetization M (measured in Tesla) and ring cross section S , once we fix the ring dimensions we may achieve tunability from the proportionality between ϕ_Z and $M(T)$. Choosing then an appropriate magnetic material with a suitable Curie-Weiss behavior, we could define a temperature interval of operation, say T_1 and T_2 , so that the magnetic flux $M(T_1)S - M(T_2)S$ increases by a factor of 2. This would provide a tunable magnetic phase plate capable of producing Zernike shifts between $\pi/2$ (higher temperature) and π (lower temperature).

Given the proportionality between magnetic flux and Zernike shift, in term of ring shape we may choose any combination of thickness and width of the ring that satisfies

$$\frac{\phi_0}{4R_2^2 M(T)} \leq \tau(1 - \sigma) \leq \frac{\phi_0}{2R_2^2 M(T)} \quad (2)$$

where $\tau = t/2R_2$ and $\sigma = R_1/R_2$ are the dimensionless shape parameters of the ring. To give an example, suppose we choose to fabricate the phase plate with some yet unidentified Iron compound that has a Curie point around 600 K. Its saturation magnetization at $T=0$ might be, hypothetically, 2 T. If we choose T_1 at room temperature we may expect from a rough mean-field estimate a magnetization around $M(T_1) \sim 1.7$ T. Choosing T_2 just below the Curie point, e.g. $T_2/T_c = 0.9$, we expect $M(T_2) \sim 0.85$ T. We could then adjust the Zernike shift by $\pi/2$ as we vary the temperature in a 240 K wide range, which does not seem to require extensive technical efforts to be implemented in a microscope.

With such material and temperature range chosen, we now illustrate what the geometrical constrain would dictate. Suppose we fabricate rings with $R_2 = 150$ nm, which is a reasonable compromise between current patterning capabilities and electron-optical requirements of having the smallest possible hole. Equation (2) now reads $0.0177 \leq \tau(1 - \sigma) \leq 0.0354$, so that we are free to choose thickness t and width ($R_2 - R_1$) accordingly. For instance, if we set $(R_2 - R_1) = 50$ nm, which is well within patterning capabilities, we have $\sigma = 2/3$ and a thickness constrained to $16 \leq t \leq 32$ (in nm).

4. Vortex state statistical occurrence

As a preliminary exploration of this parameter space, we aimed at developing some feeling on the likelihood of finding a stable vortex state using micromagnetic simulations [11]. We found a variety of competing states, the occurrence of which depends strongly on the input parameters of the simulations. Figure 2 shows four observed states: onion, horseshoe vortex and non-vortex. In this case, variety is a problem, as ideally we would like a set of shape parameters, compatible with the geometrical constraints, that results in 100% vortex occurrence. A possibility worth considering is to employ non-circular rings, such as pentagons. The presence of corners, smooth or sharp as they may be depending on patterning resolution during fabrication, may have an effect in the occurrence and stability of vortices. To explore this perspective, we have compared the statistics of vortex occurrence in circular and pentagonal rings starting with the same initial condition of random magnetization. The results are

shown in Fig. 2, where a clear statistical improvement is observable for pentagonal rings: almost half (48%) of the simulations terminated in a vortex state (versus 30% for circular rings), with the remaining three states divided unevenly. In comparison, the statistic for circular rings is almost uniformly distributed over the four states.

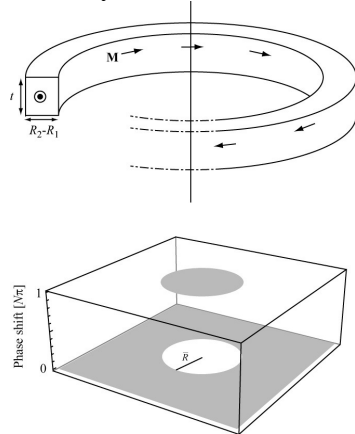


Figure 1. A magnetized ring acting as a phase plate.

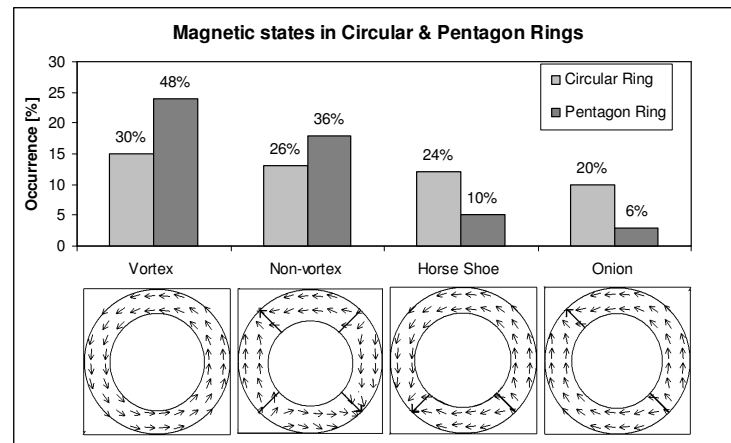


Figure 2. Statistics of vortex occurrence from random initial magnetization in circular and pentagonal rings.

There are two additional advantages in pentagonal rings: i) an enlargement of the region in parameter space where a vortex state is expected, which will be discussed in the next section, and ii) the possibility of restoring vortex states by application of a suitable external field, something that is prevented by the symmetry of a circular ring. The presence of corners, acting as pinning sites for domain wall motion, enables us to apply a suitable set of in-plane external fields and turn any non-vortex into vortex states. This analysis will be the subject of future efforts.

5. The magnetic phase diagram

A theoretical phase boundary separating the expected occurrence of in-plane and vortex states in circular rings as we vary the shape parameters (σ, τ) was derived in [10]. However, the simplified considerations therein turned out to be a rough underestimate of a realistic curve, such as one obtained by micromagnetic simulations. The likely reason is that the metastable onion state is located around a deep local minimum of the energy landscape, and it may not be possible for a system with a given magnetic history and at a certain finite temperature to overcome the barriers separating the metastable (onion) and ground (vortex) states.

To establish the operational region of magnetic phase plates, we have calculated a phase diagram through micromagnetic simulations [11] on rings with different shape parameters. Simulations are carried out with the following choice of fixed parameters: Iron ($A=21$ pJ/m, $M_S=2.15$ T), damping parameter $\alpha=0.1$, crystal anisotropy was set to 0 to mimic a polycrystalline ring, outer radius of the ring $R_2=150$ nm, uniform initial magnetization. From the simulations, we derive simulated phase boundaries that are expected to be more realistic than the idealized theoretical curves presented in Ref. [10]. Simulations were carried out varying the two aspect ratios τ and σ . For every value of σ (which requires a different mask in the LLG simulation software), we increased the thickness progressively until a vortex state was obtained. The aspect ratio τ of the first simulation producing a vortex was assigned to the phase boundary. Further increase of τ always resulted in a vortex. Results are shown in Fig. 3, where we observe that, for pentagonal rings (circles), a substantial fraction of the operational domain (dark shade of grey) identified by the geometrical constraint, equation (2), is compatible with the expectation of a vortex. The curve corresponding to circular rings (squares) is substantially higher in the phase diagram, so that a smaller portion of the operational domain (C+P) is available.

With pentagonal rings, we observe that the phase boundary lies around smaller values of τ . For example, when $\tau=0.04$, we expect a vortex in pentagonal rings, whereas in circular rings we do not. We also observe that, in both circular and pentagonal rings, as σ approaches 1 (thin shell), vortex occurrence seems to lose its dependence on σ . However, for pentagonal rings, most of the phase boundary is actually almost flat (little σ -dependence). We observe that after a critical τ value, any change in σ no longer influences or determines the vortex formation. This may grant us a bit of extra freedom in designing and fabricating a phase plate, as the role of the inner diameter appears not critical. Overall, we note a sizeable enlargement of the constraint-compatible (σ, τ) -region where vortex occurrence is expected, thus favouring the choice of pentagonal over circular rings.

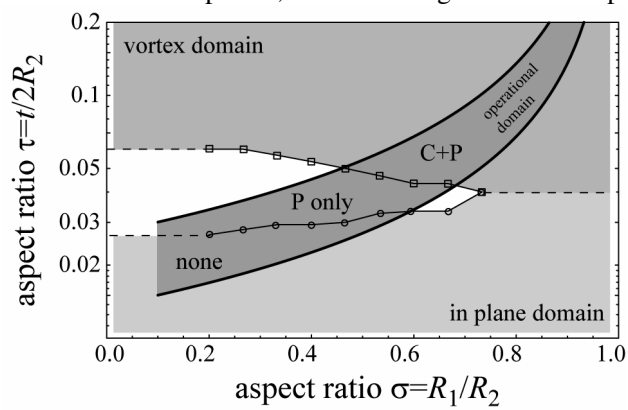


Figure 2. Numerical phase boundary separating vortex and in-plane/onion domains for circular (C) and pentagonal (P) rings. The operational region resulting from geometrical constraints is bounded between the two curves calculated from equation (2) for the hypothetical material as described in the text.

6. Conclusions

In this paper we have analyzed rings that may be potentially employed in the development of tunable magnetic phase plates. LLG simulations and analysis reveal that i) a useful operation domain exists in the (σ, τ) plane compatible with geometrical constraints; ii) the operational domain appears larger when pentagonal rings are examined, suggesting a higher degree of freedom in the choice of shape parameters; iii) the statistical occurrence of the vortex state is more favourable with pentagonal rings; iv) the asymmetry of pentagonal rings results in a sensitivity to in-plane applied field (absent in circular rings) that open a pathway for restoring a vortex from a non-vortex state. From the analysis and simulations carried out on both the circular and noncircular rings, pentagon shape rings emerge as the most favored for the phase plate development. A strategy for vortex state restoration that relies solely on in-plane applied fields is the subject of our current efforts, and will be reported elsewhere.

References

- [1] Zhu J, Zheng Y and Prinz G A 2000 *J. Appl. Phys.* **87** 6668
- [2] Kikkawa J M and Awschalom D D 1999, *Nature* **397** 139
- [3] Hosokawa F, Danev R, Arai, Y and Nagayama K 2005 *J. Electron Microsc.* **54** 317
- [4] Lentzen M 2004 *Ultramicroscopy* **99** 211
- [5] Gamm B, Schultheiß K, Gerthsen D and Schröder R R 2007 *Ultramicroscopy* **108** 878
- [6] Malac M, Beleggia M, Taniguchi Y, Egerton R F and Zhu Y 2008 *Ultramicroscopy* **109** 14
- [7] Volkl E, Allard L and Joy D C (editors) 1999 *Introduction to Electron Holography* (New York: Kluwer Academic) pp 211-217
- [8] Beleggia M 2008 *Ultramicroscopy* **108** 953
- [9] Majorovits E, Barton B, Schultheiß K, Pérez-Willard F, Gerthsen D and Schröder R 2007 *Ultramicroscopy* **107** 213
- [10] Beleggia M, Lau J W, Schofield M A, Zhu Y, Tandon S and De Graef M 2006 *J. Magn. Mater.* **301** 131
- [11] Scheinfein M R and Price E A 2003 *LLG User Manual v2.50* (llgmicro@mindspring.com)